Graphical Abstract

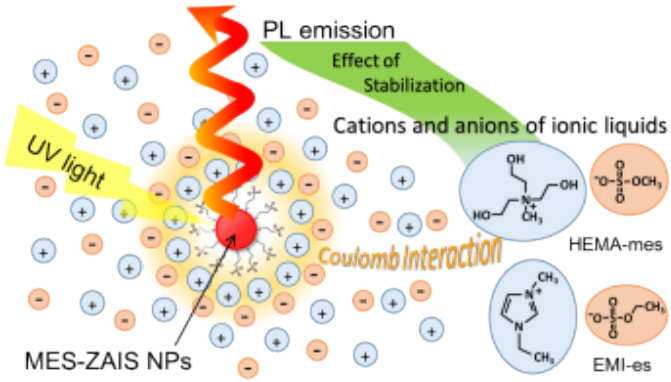

Improvement of Photoluminescence Stability of ZnS-$AgInS_2$ Nanoparticles through Interactions with Ionic Liquids

Shushi Suzuki,[*†] *Yuuki Hattori*,[†] *Susumu Kuwabata*,[§]*and Tsukasa Torimoto*[*†]

[†]Graduate School of Engineering, Nagoya University, Furo-cho, Chikusa-ku, Nagoya 464-8603, Japan

[§]Graduate School of Engineering, Osaka University, Suita, Osaka 565-0871, Japan

AUTHOR INFORMATION

Corresponding Author

*Shushi Suzuki and *Tsukasa Torimoto,

Graduate School of Engineering, Nagoya University, Furo-cho, Chikusa-ku, Nagoya 464-8603, Japan

Fax: +81-52-789-5299; Tel.: +81-52-789-2587;

E-mail: shushi@apchem.nagoya-u.ac.jp, torimoto@apchem.nagoya-u.ac.jp

ABSTRACT

Photoluminescence (PL) stability of ZnS-$AgInS_2$ (ZAIS) nanoparticles (NPs) prepared via thermal decomposition of $(AgIn)_xZn_{2(1-x)}(S_2CN(C_2H_5)_2)_4$ (x=0.5, 0.8 and 1.0) was improved by ionic liquids (ILs) of 1-ethyl-3-metylimidazolium ethylsulfate (EMI-es) and tris (2-hydroxyethyl) methylammonium methylsulfate (HEMA-mes). Through ligand exchange processes from oleylamine (OLA) to sodium 2-mercaptoethanesulfonic acid (MES), hydrophilic NP's surfaces changed into hydrophobic ones, resulting in that the ZAIS NPs could be dispersed in the ILs. UV irradiation caused the PL deterioration of ZAIS NPs in solutions, but MES-ZAIS NPs in the ILs exhibited higher PL stability than the OLA-ZAIS NPs in chloroform, the degree being more remarkable for NPs dispersed in HEMA-mes than in EMI-es. The improvement of PL stability could be interpreted as a result of stabilization of MES adsorbed on the NPs through electrostatic interaction between MES and the ILs. Exposing to the air and mixing with the water accelerated the PL deterioration of the NPs.

KEYWORDS Photoluminescent (PL) stability; ZnS-$AgInS_2$ (ZAIS) NPs; capping ligands; ionic liquids; electrostatic interaction

1. INTRODUCTION

Ionic liquids (ILs) are attractive substances, in which positive and negative ions of molecules interacted with each other electrostatically, resulting in a liquid state at room temperature as a salt. One of the usages of ILs was a medium for dispersing nanoparticles (NPs) without adding stabilized agents of organic molecules. For example, metal and metal oxide NPs dispersed in ILs were synthesized with high stability by sputter-deposition techniques[1-7]. Encapsulation of the NPs in cations and anions of the ILs through van der Waals and electrostatic interactions results in highly stable states of NPs, as summarized in the previous review papers[8, 9]. Another characteristic of ILs as solvents for retarding degradation of NP's functions has been reported. The photoluminescent (PL) stability of the semiconductor NPs of CdS[10-12], CdSe[13-15] and CdTe[16-20] could be improved by ILs when the NPs were incorporated in ILs. For instance, the PL property of the CdTe NPs dispersed in 1-butyl-3-methylimidazolium bis(trifluoromethanesulfonyl) amide (BMI-TFSA) retained its original intensity at least for 2 h[16]. The effect was interpreted as that ILs have the extremely high salt concentration (ca. 7 mol dm^{-3} in ions) which suppresses the Coulombic repulsion with positive charges on capping ligands of thiocholine bromide (TCB) adsorbed on the NPs, resulting in the efficient stability of the NPs under UV light irradiation[16, 17].

Those previous studies on the incorporation of semiconductor NPs showed a further potential of ILs as colored or luminescent fluids. However, high toxicity of Cd-contained fluids is not adequate for wide applications. Among semiconductor NPs, ZnS-$AgInS_2$ (ZAIS) and $AgInS_2$ (AIS) NPs are highly attractive luminescent nanomaterials, because of relatively less toxicity[21-28]. These NPs prepared from a precursor of $(AgIn)_xZn_{2(1-x)}(S_2CN(C_2H_5)_2)_4$ (x=

0-1) can change their PL colors from blue-green to dark red with increasing in *x* of the precursor. The PL emission mechanism of ZAIS NPs can be understood by donor−acceptor (D−A) transition through defect states natively created in a bulk during synthesis of the NPs. The native defects are known to involve 'sulfur vacancy/interstitial silver' acting as donors and 'silver vacancy/interstitial sulfur' acting as acceptors at deep levels[29]. On the other hand, surface defects or trap states were considered as a cause of reducing the PL emission intensity through nonradiative recombination of charge carriers. It was proposed that capping ligands of dodecanethiol molecules on the NPs suppressed charge recombination by surface passivation of AIS NPs[26, 30], leading to improvements of the PL property.

Therefore, increasing the stability of the capping ligands on the NPs is crucial to improving the PL stability of the NPs, as mentioned earlier on mixing ILs with CdS[10-12], CdSe[13-15] and CdTe[16-20] NPs. For the ZAIS NPs and the AIS NPs, a few studies were only reported about the improvement of PL stability using polymers served as capping agents[31, 32], instead of ILs. Using methacrylate resin[31], the AIS NPs retained almost initial PL property after 1000 h of exposing to the UV light (365 nm, 2.3 mW cm^{-2} at a sample position). In the same way, the ZAIS NPs (x = 0.6) in the resin took 1000 h until the PL intensity decreased by half under the light irradiation (450 nm, 4 mW cm^{-2} at a sample position). Using a gelatin matrix[32], the ZnS coated-AIS NPs showed PL emission for at least 3 h during UV light irradiation (365 nm, using a 50 W pulsed xenon lamp). In those studies, polymers around the NPs could change the PL stability. However, there has been no study using ILs on the PL stability of the ZAIS NPs and the AIS NPs. The present study shows an application

of ILs to improve the PL stability of these NPs. The effect of ILs on the PL stability is discussed, as well as influences of exposing to the air and mixing of water.

2. EXPERIMENTAL

2.1 Preparation of ZAIS NPs and AIS NPs dispersed in ILs. The PL stability of the ZAIS NPs dispersed in ILs were evaluated as follows. First, the ZAIS NPs capped with oleylamine (OLA) in chloroform were synthesized[22, 33], followed by replacing OLA with sodium 2-mercaptoethanesulfonic acid (MES) to make the NPs being water-soluble [33]; the obtained-NPs were described as the MES-ZAIS NPs. Next, the MES-ZAIS NPs were re-precipitated by adding ethanol, then a mixture of NPs with ILs was obtained by introducing the IL of 1-ethyl-3-metylimidazolium ethylsulfate (EMI-es; Tokyo Chemical Industry Co. Ltd.) or tris (2-hydroxyethyl) methylammonium methylsulfate (HEMA-mes; Sigma-Aldrich Co. LLC.). Molecular structures of EMI-es and HEMA-mes were listed in Fig. S1 as supporting information. Six kinds of pellucid mixtures were totally obtained for each IL with chemical compositions of the ZAIS (x=0.5 and 0.8) NPs and the AIS (x=1.0) NPs. These ILs were dried for at least 3 h at 393 K under vacuum conditions before use. As shown in Fig. S2, the PL properties of the AIS NPs were not significantly influenced by replacing the solvents from water to the ILs, since the PL properties of the AIS NPs were only changed as a small peak-shifting and/or a small peak-broadening

2.2 Characterizations. PL spectra were acquired using 10-mm path-length quartz cuvettes with a photonic multichannel analyzer, PMA-12 (Hamamatsu Photonics K.K.) by monochromatic light irradiation (λ = 365 nm) at room temperature. The absorbance of the NPs in a quartz cuvette was adjusted to be 1.0 at 365 nm in wavelength in the absorption spectra, obtained by a UV-visible spectrophotometer, Agilent/HP 8453A (Agilent Technology, Inc.). The atmosphere in the cuvette was replaced with nitrogen by bubbling before spectroscopic measurements except for the case examining the influence of exposing to the air. The PL stability of the NPs was estimated from time-evolved intensities in the PL spectra measured at intervals between UV light irradiation processes. A Xe lamp, BA-X300 (USHIO Inc.) was used for the UV light source. Monochromatic light at 360 nm was obtained by passing the lamp light through interference filters with a light intensity of about 30 mW cm^{-2} at a sample position. Morphologies of the NPs were observed by a transmission electron microscope (TEM), H7650 (Hitachi, Co. Ltd.) with an acceleration voltage at 100 kV. TEM samples were prepared by dropping a droplet of ILs involving the NPs onto a carbon-coated copper grid (#10-1012, Okenshoji Co. Ltd.), followed by a rinse in water to remove excess amounts of the hydrophilic ILs with subsequent drying *in vacuo*. Particle sizes were determined using image analysis software such as ImageJ developed at the National Institutes of Health (NIH).

3. RESULTS AND DISCUSSION

Fig. 1(a)-(d) show the absorption and PL spectra on OLA-AIS NPs in chloroform, MES-AIS NPs in water, MES-AIS NPs in EMI-es, and MES-AIS NPs in HEMA-mes. The PL spectra were measured after UV irradiation for certain hours indicated in the figures, as well as the absorption spectra obtained for the initial and the final states of NPs through the measurements. The PL intensities were normalized at maxima in each series of spectra. Though the PL intensities increased tentatively to maxima in the early period of UV light irradiation, the increase might be unrelated to the IL's nature because the similar phenomenon was found in each figure. However, the PL stability of AIS NPs strongly depended on the solvents. As shown in Fig 1(a), the PL intensity for the OLA-AIS NPs in chloroform decreased to almost zero at 8 h. For the MES-AIS NPs in water, complete PL quenching was confirmed until 1.5 h in Fig. 1(b). The intensities of absorption spectra were normalized by the intensity at 360 nm in each figure. In Fig. 1(a) and (b), the absorbance in a whole wavelength region were increased after the PL quenching. Generally, the increasing of absorbance indicates particle-size growth. Thus, particle aggregation occurred

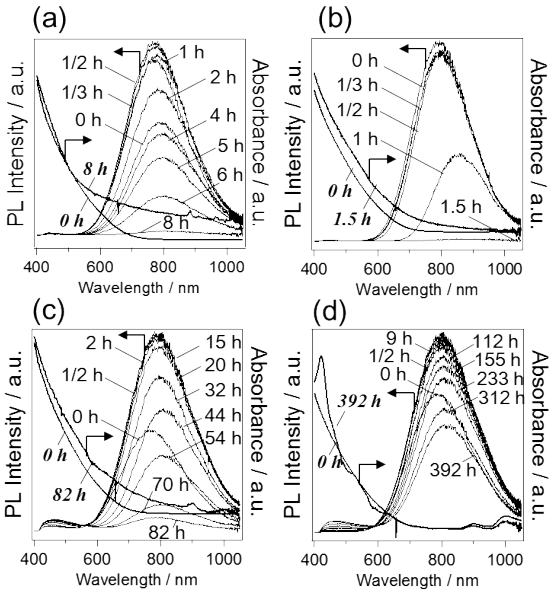

Figure 1. Absorption and PL spectra of AIS (x=1.0) NPs of (a) OLA-AIS in chloroform, (b) MES-AIS in water, (c) MES-AIS in EMI-es, and (d) MES-AIS in HEMA-mes. Notation of time in hour is total time of UV irradiation for each spectrum. The notations for absorption and PL spectra were indicated, respectively.

during the PL quenching processes. As discussed in the latter section, the aggregation was also confirmed by TEM observations. On the other hand, the normalized PL intensities for the MES-AIS NPs in EMI-es were still observed as 0.07 at 82 h in Fig. 1(c), and that for the MES-AIS NPs in HEMA-mes were observed as 0.52 at 392 h in Fig. 1 (d). As was seen in Fig. 1(a) and (b), the absorbance in a whole wavelength region in Fig. 1(c) was also increased, indicating that particle aggregation occurred. Although a peak appeared at 420 nm in Fig. 1(d), the absorbance was not changed in the almost whole wavelength region, indicating that particle aggregation did not occur significantly. As for the peak at 420 nm, it can be deduced that HEMA-mes might be decomposed partially by a long term of UV-light irradiation over 100 h, changing features of the absorption spectrum. From the results in Fig. 1(c) and 1(d), it was clearly shown that the PL stability of the AIS NPs dispersed in the ILs was improved. Figures 2 summarized time-evolved peak intensities of the PL spectra on the MES-ZAIS (x=0.5 and 0.8) NPs and the MES-AIS (x=1.0) NPs in the ILs and in the water. The normalized-intensities by maxima were plotted as a function of time by the hour for the indicated x values. Compared with the NPs in the water, the NPs in every case showed high PL stability. As were presented in Fig. 2, the PL intensities for the ZAIS NPs (x=0.5 and 0.8)

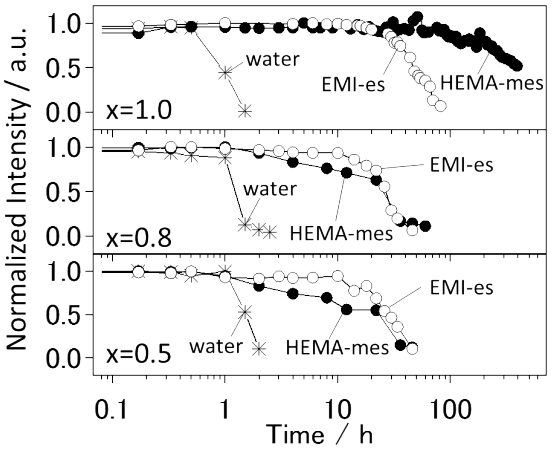

Figure 2. time-dependent change of PL intensity obtained for MES-ZAIS (x=0.5, 0.8, and 1.0) NPs in the ILs and in water. Opened marks, filled marks, and asterisk marks indicate data for EMI-es, for HEMA-mes, and for water, respectively. For logarithmic display format of time, data at 0 h are not plotted.

in both ILs were completely quenched until 50 h while the peak intensities for x=1.0 were not quenched in the same way. The PL stability improvement was prominently observed for the MES-AIS NPs in HEMA-mes, and the quenching could be roughly estimated at ca. 800 h by linear extrapolation. Thus, the PL stability was influenced by the chemical compositions of the NPs, as well as the kinds of ILs.

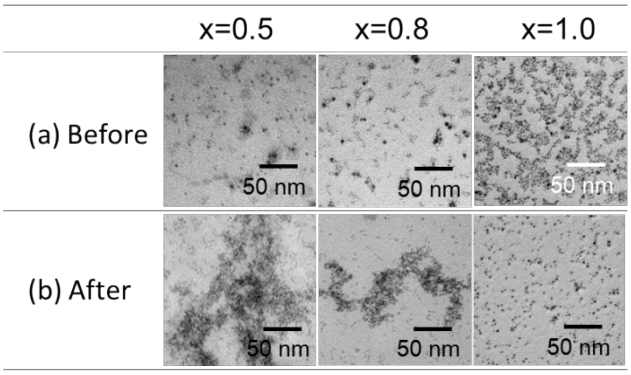

Figure 3. TEM images of ZAIS NPs (x=0.5, 0.8 and 1.0) capped with MES in HEMA-mes (a) before starting the UV light irradiation for the PL stability measurements and (b) after the measurements.

Fig. 3 shows TEM images of the MES-ZAIS (x=0.5 and 0.8) NPs and the MES-AIS (x=1.0) NPs isolated from HEMA-mes before and after the measurements of PL stability. As shown in Fig. 3(a), the initial states of NPs were well-dispersed in HEMA-mes without particle-aggregation. Their average size of NPs was within the range of 4.0–5.2 nm in diameter, estimated from the particle size distribution. For MES-ZAIS NPs in EMI-es and OLA-ZAIS NPs in chloroform, the NPs showed the same order of average sizes, as summarized in Fig. S3. After the PL stability measurements in Fig. 3(b), particle aggregations were observed for the MES-ZAIS (x=0.5 and 0.8) NPs, while no aggregation was observed for MES-AIS (x=1.0) NPs, as was expected in Fig. 1(d). It was confirmed that the PL quenching occurred with the particle aggregation.

Although the PL stability was improved in the nitrogen atmosphere, the effect of improvement was suppressed by exposing to the air. Without replacing the air into nitrogen gas in the cuvettes during the measurements, the PL stability of the NPs was lower than that of the NPs under nitrogen gas. Fig. 4(a) shows time-evolved PL peak intensity profiles of the MES-AIS NPs (x=1.0) in HEMA-mes (i) in the air and (ii) under nitrogen gas. Before the measurement of (i), a sample was pre-treated by bubbling the air sufficiently. The PL intensity in the profile of (i) decreased to 0.5 until 175 h, which is less than half of the duration of 382 h in the profile of (ii), indicating that the PL stability of NPs in the IL was deteriorated by the presence of air. In fact, the influence of oxygen on the PL stability was already pointed out in the previous studies on CdS/CdSe NPs[34-37], PbS/PbSe NPs[38, 39], although ILs were not used. Our recent study reported the size-selective photoetching process of the MES-AIS NPs in solution, suggesting that the holes in metal sulfide particles oxidized themselves[40]. The photoetching in the presence of oxygen for chalcogenides is a well-known process, where the recombination of electron-hole pairs can be prohibited by removing the electron by oxygen, and the remaining hole can be used to dissolve the chalcogenides themselves with producing SO_4^{2-} [41-43]. Further our study showed that indium oxide NPs could be prepared in ILs such as EMI-tetrafluoroborate (BF_4) through sputter-deposition with subsequent exposure to the air[3]. From these facts, it could be deduced that the MES-AIS NPs was partially oxidized even in HEMA-mes, resulting in the PL quenching.

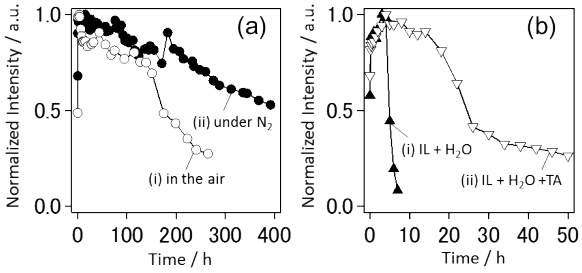

Figure 4. (a) PL stability measurements of MES-AIS NPs in HEMA-mes (i) in the air (filled circles) and (ii) under nitrogen gas (open circles). (b) PL stability measurements of MES-AIS NPs in HEMA-mes containing (i) 20 vol.% of water (filled triangles) and (ii) 20 vol.% of water with triethanolamine, TEOA (open reverse triangles). Both of them in (b) were measured under nitrogen gas.

In a similar manner, the influence of water was examined, as shown in Fig. 4(b). A profile of (i) shows a time-evolved PL peak intensity profile measured under nitrogen gas for a sample of the MES-AIS NPs in HEMA-mes by adding 20 vol.% of water. Compared with the profile (ii) in Fig. 4(a) for the case without adding water, the PL stability was significantly deteriorated by adding water. In a strict sense, water in HEMA-mes might not be removed completely in the case of Fig. 4(a), because of the hydrophilicity of ILs. The previous paper showed that the water concentration in HEMA-mes gradually increased up to less than 3 weight % after 5 h by exposing to atmosphere at 293 K and 50% atmospheric relative humidity[44]. A possibility of reaching a similar concentration of water in HEMA-mes might not be excluded even in the nitrogen atmosphere in our experiments. Nevertheless, the normalized PL intensity in the case of adding water in Fig. 4(b) decreased to 0.5 until 5 h, and the PL quenching occurred within 10 h, indicating that water surely affected negatively the PL stability improvement. Indeed, it is reasonably explained that water disrupted to form the Coulombic interaction to stabilize MES on the NPs by decreasing the concentration of ILs. Water might form the hydrogen bonding with MES, instead of the hydroxyl groups in the cations of HEMA-mes, i.e. replacing the ILs into water might decrease the PL stability.

Hence, it was confirmed that a dried environment was preferable for the PL stability improvement. Nevertheless, the PL stability could be improved again by adding a small amount of triethanolamine (TEOA). As shown in Fig. S1(c), TEOA, which is a triol molecule containing three alcohol groups like the cation of HEMA-mes, can be used as a hole scavenger. The profile (ii) in Fig. 4(b) shows a time-evolved PL peak intensity profile for a sample prepared by adding 5 wt% of TEOA to the MES-AIS NPs in HEMA-mes containing 20 vol.% of water. The PL intensity was still observed at 50 h of UV light irradiation, indicating that the decay of PL intensity was slower than that in the profile of (i) for the case without TEOA. The results exhibited that TEOA affected positively the PL stability improvement in contrast to the effect of water. The most acceptable interpretation could be elucidated that TEOA was employed as a hole scavenger to suppress the dissolution of NPs.

A plausible mechanism for the effect of ILs on the PL stability improvement was considered as follows. In the previous studies on CdSe[16, 17], two possible mechanisms were already proposed for the candidates. One is suppression of the Coulombic repulsion between functional groups of capping ligands on the NPs, resulting in increasing stability of capping ligands on the NPs. Another is the less solubility of the capping ligands to ILs, resulting in suppressing desorption of capping ligands from the NPs. In our study, since MES can be dissolved into both ILs of EMI-es and HEMA-mes, the possibility of the latter is excluded. Hence, the former can be applied to explain our results; Coulombic repulsion between the negative charges on sulfonic groups of MES was effectively compensated by positive charges on the cations of ILs through electrostatic interactions among ions, leading to being higher stable adsorption states of MES on the NPs in the ILs than that in OLA and water.

The difference in the PL stability improvement between the ZAIS (x=0.5 and 0.8) NPs and AIS (x=1.0) NPs was shown in Fig. 2. Deducing from the results on TEOA with the AIS NPs, the dissolution of ZAIS NPs might occur with higher reaction rate than that for the AIS NPs, because the ZAIS NPs were aggregated after the experiments, as shown in Fig. 3. As was previously reported, the tendency was similar to the photocatalytic activity of the H_2 evolution on the ZAIS NPs in the presence of S^{2-} as a hole scavenger[45]. Indeed, the ZAIS (x=0.5 and 0.8) NPs showed higher photocatalytic H_2 evolution rate than the AIS (x=1.0) NPs, on which the mechanism was explained that the photocatalytic activity decreased with increasing gap energy in the band structure of those NPs. It could be deduced that the low photocatalytic activity can be attributed to the low absorption rate of UV light, resulting in the low dissolution rate. Thus, the lower photocatalytic activity of the AIS NPs might be advantageous to maintaining the PL stability of the NPs even in the ILs.

In addition, the AIS (x=1.0) NPs was more stabilized by HEMA-mes than EMI-es. The effect of ILs was different in the improvement of PL stability, although such difference was not clearly observed for the ZAIS (x=0.5 and 0.8) NPs. Thus, the difference in the effect of ILs might appear on the premise of the high PL stability, or low photocatalytic activity. By an analogy with TEOA, a mechanism of electron- or hole-scavenging by the ILs to suppress the dissolution of the NPs could be considered. The NPs could donate electrons or holes to adjacent cations and anions of the ILs, if the energy levels for the molecular orbitals of ILs are close to the positions of electronic band edges in the NPs. Although the electronic state calculations should be required for proving the idea, it was expected that the energy level of molecular orbitals for HEMA-mes might be closer to the position of the band edge in the

band structures of the AIS NPs, compared with those for EMI-es, resulting in the high PL stability.

In another way, the difference in the effect of ILs could be considered from the molecular structures. Comparing the ILs, there are structural difference between cations, as shown in Fig. S1. The cation of EMI-es has an aromatic imidazolium ring, while the cation of HEMA-mes has an aliphatic chain containing three hydroxyl groups. As discussed in the above, the Coulomb repulsion compensation was expected to increase when the cations of ILs approached to the MES adsorbed on the AIS NPs, although the density of cations around the NPs increased and steric hindrance might become enlarged among cations. Thus, smaller size of cations was preferable to achieve a higher degree of Coulomb repulsion compensation. Besides, hydrogen bond formation was also expected between the hydroxyls in the structure of HEMA-mes and MES on the NPs. Such hydrogen bond interaction might assist the approaching of cations to the NPs, leading to more effective compensation states of Coulomb repulsion, compared with the case of EMI-es.

4. CONCLUSIONS

The study shows that the Photoluminescence (PL) stability for the sodium 2-mercaptoethanesulfonic acid capped ZnS-$AgInS_2$ (MES-ZAIS) nanoparticles (NPs) was improved by the ionic liquids (ILs) of 1-ethyl-3-metylimidazolium ethylsulfate (EMI-es) and tris (2-hydroxyethyl) methylammonium methylsulfate (HEMA-mes). The effect of HEMA-

mes was higher than the effect of EMI-es. The chemical composition of ZAIS NPs also affected the improvement of PL stability in the ILs. The effect of ILs can be deduced as charge compensation of the Coulomb repulsion between the negative charges on MES on the NPs and the positive charges on the cations of ILs, as suggested previously. Besides, the air and water were recognized as inhibitors to elongate the PL stability through disruption of the above interactions between MES and the ILs. Forming the properly-stable state with electrostatic interactions between capping ligands on the NPs and ILs was crucial for the improvement of PL stability by the ILs.

ASSOCIATED CONTENT

Supporting Information

1. Molecular structures of ionic liquids used in the experiments about 1-ethyl-3-methylimidazolium ethylsulfate (EMI-es), tris(2-hydroxyethyl)methyl ammonium methylsulfate (HEMA-mes), and triethanolamine which provided pellucid mixed solutions with the MES-ZAIS NPs. (SI_1_Suzuki_NagoyaU.pdf)

2. Particle size distributions data of ZAIS NPs (x=0.5, 0.8 and 1.0) collected from TEM observations of corresponded NPs. (SI_2_Suzuki_NagoyaU.pdf)

AUTHOR INFORMATION

Corresponding Authors

*E-mail: shushi@apchem.nagoya-u.ac.jp

*E-mail: torimoto@apchem.nagoya-u.ac.jp

NOTES

The authors declare no competing financial interests.

ACKNOWLEDGEMENT

This work is supported from Japan Society for the Promotion of Science (JSPS) by a Grant-in-Aid for Scientific Research (C) (Number: 25390079), a Grant-in- Scientific Research on Innovative Areas “Photosynergetics” (Number: JP15H01082), a Grant-in- Scientific Research on Innovative Areas “Nano-Material” from the JSPS (Number: JP16H06507), and a Funding Program for Next Generation World-Leading Research (NEXT Program) (No. GR054).

REFERENCES

[1] T. Torimoto, K. Okazaki, T. Kiyama, K. Hirahara, N. Tanaka, S. Kuwabata, Sputter deposition onto ionic liquids: Simple and clean synthesis of highly dispersed ultrafine metal nanoparticles, Appl. Phys. Lett., 89 (2006) 243117.

[2] Y. Hatakeyama, M. Okamoto, T. Torimoto, S. Kuwabata, K. Nishikawa, Small-Angle X-ray Scattering Study of Au Nanoparticles Dispersed in the Ionic Liquids 1-Alkyl-3-methylimidazolium Tetrafluoroborate, J. Phys. Chem. C, 113 (2009) 3917-3922.

[3] T. Suzuki, K. Okazaki, S. Suzuki, T. Shibayama, S. Kuwabata, T. Torimoto, Nanosize-Controlled Syntheses of Indium Metal Particles and Hollow Indium Oxide Particles via the Sputter Deposition Technique in Ionic Liquids, Chem. Mater., 22 (2010) 5209-5215.

[4] H. Wender, L.F. de Oliveira, P. Migowski, A.F. Feil, E. Lissner, M.H.G. Prechtl, S.R. Teixeira, J. Dupont, Ionic Liquid Surface Composition Controls the Size of Gold

Nanoparticles Prepared by Sputtering Deposition, J. Phys. Chem. C, 114 (2010) 11764-11768.
[5] S. Suzuki, T. Suzuki, Y. Tomita, M. Hirano, K. Okazaki, S. Kuwabata, T. Torimoto, Compositional control of AuPt nanoparticles synthesized in ionic liquids by the sputter deposition technique, CrystEngComm, 14 (2012) 4922-4926.
[6] S. Suzuki, Y. Tomita, S. Kuwabata, T. Torimoto, Synthesis of alloy AuCu nanoparticles with the $L1_0$ structure in an ionic liquid using sputter deposition, Dalton Trans., 44 (2015) 4186-4194.
[7] D. König, K. Richter, A. Siegel, A.-V. Mudring, A. Ludwig, High-Throughput Fabrication of Au–Cu Nanoparticle Libraries by Combinatorial Sputtering in Ionic Liquids, Adv. Funct. Mater., 24 (2014) 2049-2056.
[8] J. Dupont, J.D. Scholten, On the structural and surface properties of transition-metal nanoparticles in ionic liquids, Chem. Soc. Rev., 39 (2010) 1780-1804.
[9] Z. He, P. Alexandridis, Nanoparticles in ionic liquids: interactions and organization, Phys. Chem. Chem. Phys., 17 (2015) 18238-18261.
[10] K. Biswas, C.N.R. Rao, Use of Ionic Liquids in the Synthesis of Nanocrystals and Nanorods of Semiconducting Metal Chalcogenides, Chem. Eur. J., 13 (2007) 6123-6129.
[11] K.L. Knappenberger, D.B. Wong, W. Xu, A.M. Schwartzberg, A. Wolcott, J.Z. Zhang, S.R. Leone, Excitation-Wavelength Dependence of Fluorescence Intermittency in CdSe Nanorods, Acs Nano, 2 (2008) 2143-2153.
[12] I. Mukherjee, G. Dinda, S. Ghosh, S.P. Moulik, Synthesis, characterization, and applications of microheterogeneous-templated CdS nanodispersions, J. Nanopart. Res., 14 (2012).
[13] T. Yamada, K. Goushi, A. Otomo, Time-correlated single photon counting system and light-collection system for studying fluorescence emitters under high-vacuum conditions: Use of immersion objective and ionic liquid, Thin Solid Films, 518 (2009) 432-436.
[14] E. Nuhiji, F.G. Amar, H.X. Wang, N. Byrne, T.L. Nguyen, T. Lin, Whispering gallery mode emission generated in tunable quantum dot doped glycerol/water and ionic liquid/water microdroplets formed on a superhydrophobic coating, J. Mater. Chem., 21 (2011) 10823-10828.
[15] A. Panniello, E. Binetti, C. Ingrosso, M.L. Curri, A. Agostiano, R. Tommasi, M. Striccoli, Semiconductor nanocrystals dispersed in imidazolium-based ionic liquids: a spectroscopic and morphological investigation, J. Nanopart. Res., 15 (2013).
[16] T. Nakashima, T. Kawai, Quantum dots-ionic liquid hybrids: efficient extraction of cationic CdTe nanocrystals into an ionic liquid, Chem. Commun., (2005) 1643-1645.
[17] T. Nakashima, T. Sakakibara, T. Kawai, Highly Luminescent CdTe Nanocrystal–Polymer Composites Based on Ionic Liquid, Chem. Lett., 34 (2005) 1410-1411.
[18] Y. Nonoguchi, T. Nakashima, T. Kawai, Low-Temperature Observation of Photoinduced Electron Transfer from CdTe Nanocrystals, J. Phys. Chem. C, 113 (2009) 11464-11468.

[19] Y. Hayakawa, Y. Nonoguchi, H.P. Wu, E.W.G. Diau, T. Nakashima, T. Kawai, Rapid preparation of highly luminescent CdTe nanocrystals in an ionic liquid via a microwave-assisted process, J. Mater. Chem., 21 (2011) 8849-8853.
[20] S. Patra, A. Samanta, Effect of Capping Agent and Medium on Light-Induced Variation of the Luminescence Properties of CdTe Quantum Dots: A Study Based on Fluorescence Correlation Spectroscopy, Steady State and Time-Resolved Fluorescence Techniques, J. Phys. Chem. C, 118 (2014) 18187-18196.
[21] W.M. Du, X.F. Qian, J. Yin, Q. Gong, Shape- and phase-controlled synthesis of monodisperse, single-crystalline ternary chalcogenide colloids through a convenient solution synthesis strategy, Chem. Eur. J., 13 (2007) 8840-8846.
[22] T. Torimoto, T. Adachi, K. Okazaki, M. Sakuraoka, T. Shibayama, B. Ohtani, A. Kudo, S. Kuwabata, Facile synthesis of ZnS-$AgInS_2$ solid solution nanoparticles for a color-adjustable luminophore, J. Am. Chem. Soc., 129 (2007) 12388-12389.
[23] Y. Hamanaka, T. Ogawa, M. Tsuzuki, T. Kuzuya, Photoluminescence Properties and Its Origin of $AgInS_2$ Quantum Dots with Chalcopyrite Structure, J. Phys. Chem. C, 115 (2011) 1786-1792.
[24] B.D. Mao, C.H. Chuang, J.W. Wang, C. Burda, Synthesis and Photophysical Properties of Ternary I-III-VI $AgInS_2$ Nanocrystals: Intrinsic versus Surface States, J. Phys. Chem. C, 115 (2011) 8945-8954.
[25] B.D. Mao, C.H. Chuang, F. Lu, L.X. Sang, J.J. Zhu, C. Burda, Study of the Partial Ag-to-Zn Cation Exchange in $AgInS_2$/ZnS Nanocrystals, J. Phys. Chem. C, 117 (2013) 648-656.
[26] Y. Hamanaka, T. Ogawa, M. Tsuzuki, K. Ozawa, T. Kuzuya, Luminescence properties of chalcopyrite $AgInS_2$ nanocrystals: Their origin and related electronic states, J. Lumin., 133 (2013) 121-124.
[27] W.D. Xiang, C.P. Xie, J. Wang, J.S. Zhong, X.J. Liang, H.L. Yang, L. Luo, Z.P. Chen, Studies on highly luminescent $AgInS_2$ and Ag-Zn-In-S quantum dots, J. Alloys Compd., 588 (2014) 114-121.
[28] T. Yatsui, F. Morigaki, T. Kawazoe, Controlling the optical and structural properties of ZnS-$AgInS_2$ nanocrystals by using a photo-induced process, Beilstein J. Nanotech., 5 (2014) 1767-1773.
[29] M.J. Rao, T. Shibata, S. Chattopadhyay, A. Nag, Origin of Photoluminescence and XAFS Study of $(ZnS)_{1-x}(AgInS2)_x$ Nanocrystals, J. Phys. Chem. Lett., 5 (2014) 167-173.
[30] J.Y. Chang, G.Q. Wang, C.Y. Cheng, W.X. Lin, J.C. Hsu, Strategies for photoluminescence enhancement of AgInS2 quantum dots and their application as bioimaging probes, J. Mater. Chem., 22 (2012) 10609-10618.
[31] S. Maeda, T. Uematsu, T. Doi, J. Tokuda, T. Fujita, T. Torimoto, S. Kuwabata, Long Term Optical Properties of ZnS-$AgInS_2$ and $AgInS_2$-$AgGaS_2$ Solid-Solution Semiconductor Nanoparticles Dispersed in Polymer Matrices, Electrochemistry, 79 (2011) 813-816.
[32] X. Kang, L. Huang, Y. Yang, D. Pan, Scaling up the Aqueous Synthesis of Visible Light Emitting Multinary $AgInS_2$/ZnS Core/Shell Quantum Dots, J. Phys. Chem. C, 119 (2015) 7933-7940.

[33] T. Kameyama, K.I. Okazaki, Y. Ichikawa, A. Kudo, S. Kuwabata, T. Torimoto, Photoluminescence enhancement of ZnS-$AgInS_2$ solid solution nanoparticles layer-by-layer-assembled in inorganic multilayer thin films, Chem. Lett., 37 (2008) 700-701.
[34] F. Koberling, A. Mews, T. Basché, Oxygen-Induced Blinking of Single CdSe Nanocrystals, Adv. Mater., 13 (2001) 672-676.
[35] W.G.J.H.M. van Sark, P.L.T.M. Frederix, D.J. Van den Heuvel, H.C. Gerritsen, A.A. Bol, J.N.J. van Lingen, C. de Mello Donegá, A. Meijerink, Photooxidation and Photobleaching of Single CdSe/ZnS Quantum Dots Probed by Room-Temperature Time-Resolved Spectroscopy, J. Phys. Chem. B, 105 (2001) 8281-8284.
[36] A.Y. Nazzal, X.Y. Wang, L.H. Qu, W. Yu, Y.J. Wang, X.G. Peng, M. Xiao, Environmental effects on photoluminescence of highly luminescent CdSe and CdSe/ZnS core/shell nanocrystals in polymer thin films, J. Phys. Chem. B, 108 (2004) 5507-5515.
[37] N. Durisic, A.G. Godin, D. Walters, P. Grutter, P.W. Wiseman, C.D. Heyes, Probing the "Dark" Fraction of Core-Shell Quantum Dots by Ensemble and Single Particle pH-Dependent Spectroscopy, Acs Nano, 5 (2011) 9062-9073.
[38] J.J. Peterson, T.D. Krauss, Photobrightening and photodarkening in PbS quantum dots, Phys. Chem. Chem. Phys., 8 (2006) 3851-3856.
[39] J.W. Stouwdam, J. Shan, F.C.J.M. van Veggel, A.G. Pattantyus-Abraham, J.F. Young, M. Raudsepp, Photostability of colloidal PbSe and PbSe/PbS core/shell nanocrystals in solution and in the solid state, J. Phys. Chem. C, 111 (2007) 1086-1092.
[40] T. Torimoto, M. Tada, M.L. Dai, T. Kameyama, S. Suzuki, S. Kuwabata, Tunable Photoelectrochemical Properties of Chalcopyrite $AgInS_2$ Nanoparticles Size-Controlled with a Photoetching Technique, J. Phys. Chem. C, 116 (2012) 21895-21902.
[41] A. van Dijken, A.H. Janssen, M.H.P. Smitsmans, D. Vanmaekelbergh, A. Meijerink, Size-selective photoetching of nanocrystalline semiconductor particles, Chem. Mater., 10 (1998) 3513-3522.
[42] D. Meissner, I. Lauermann, R. Memming, B. Kastening, Photoelectrochemistry of cadmium sulfide. 2. Influence of surface-state charging, The Journal of Physical Chemistry, 92 (1988) 3484-3488.
[43] D. Meissner, C. Benndorf, R. Memming, Photocorrosion of cadmium sulfide: Analysis by photoelectron spectroscopy, Appl. Surf. Sci., 27 (1987) 423-436.
[44] S. Aparicio, M. Atilhan, M. Khraisheh, R. Alcalde, Study on Hydroxylammonium-Based Ionic Liquids. I. Characterization, The Journal of Physical Chemistry B, 115 (2011) 12473-12486.
[45] T. Takahashi, A. Kudo, S. Kuwabata, A. Ishikawa, H. Ishihara, Y. Tsuboi, T. Torimoto, Plasmon-Enhanced Photoluminescence and Photocatalytic Activities of Visible-Light-Responsive ZnS-$AgInS_2$ Solid Solution Nanoparticles, J. Phys. Chem. C, 117 (2013) 2511-2520.

FIGURE CAPTIONS

Figure 1. Absorption and PL spectra of AIS (x=1.0) NPs of (a) OLA-AIS in chloroform, (b) MES-AIS in water, (c) MES-AIS in EMI-es, and (d) MES-AIS in HEMA-mes. Notation of time in hour is total time of UV irradiation for each spectrum. The notations for absorption and PL spectra were indicated, respectively.

Figure 2. time-dependent change of PL intensity obtained for MES-ZAIS (x=0.5, 0.8, and 1.0) NPs in the ILs and in water. Opened marks, filled marks, and asterisk marks indicate data for EMI-es, for HEMA-mes, and for water, respectively. For logarithmic display format of time, data at 0 h are not plotted.

Figure 3. TEM images of ZAIS NPs (x=0.5, 0.8 and 1.0) capped with MES in HEMA-mes (a) before starting the UV light irradiation for the PL stability measurements and (b) after the measurements.

Figure 4. (a) PL stability measurements of MES-AIS NPs in HEMA-mes (i) in the air (filled circles) and (ii) under nitrogen gas (open circles). (b) PL stability measurements of MES-AIS NPs in HEMA-mes containing (i) 20 vol.% of water (filled triangles) and (ii) 20 vol.% of water with triethanolamine, TEOA (open reverse triangles). Both of them in (b) were measured under nitrogen gas.

Figure S1. Molecular structures of ILs which were applied for the experiments: (a) 1-ethyl-3-methylimidazolium ethylsulfate (EMI-es), (b) tris(2-hydroxyethyl)methyl ammonium methylsulfate (HEMA-mes), (c) Triethanolamine

Figure S2. (a) PL spectra of (i) MES-AIS NPs in water (dotted line), (ii) MES-AIS NPs in EMI-es (solid line), and (iii) their differential spectrum. (b) PL spectra of (i) MES-AIS NPs in water (dotted line), (ii) MES-AIS NPs in HEMA-mes (solid line), and (iii) their differential spectrum. (c) Absorption spectra of (i) EMI-es (solid line), and (ii) HEMA-mes(dotted line).

Figure S3. Particle size distributions of ZAIS NPs (x=0.5, 0.8) and AIS NPs (x=1.0) capped with MES in (a) EMI-es, (b) HEMA-mes, and (c) the NPs capped with OLA in chloroform. All the data were estimated from TEM observations, observed before the experiments on the PL stability enhancement.

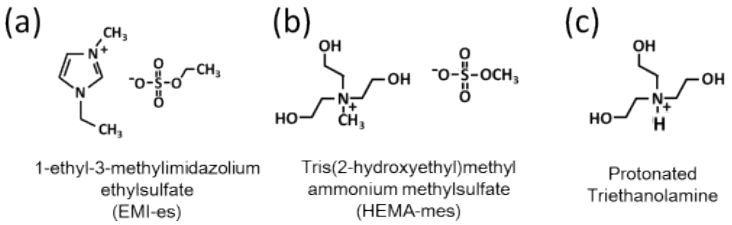

Figure S1. Molecular structures of ILs which were applied for the experiments: (a) 1-ethyl-3-methylimidazolium ethylsulfate (EMI-es), (b) tris(2-hydroxyethyl)methyl ammonium methylsulfate (HEMA-mes), (c) Triethanolamine

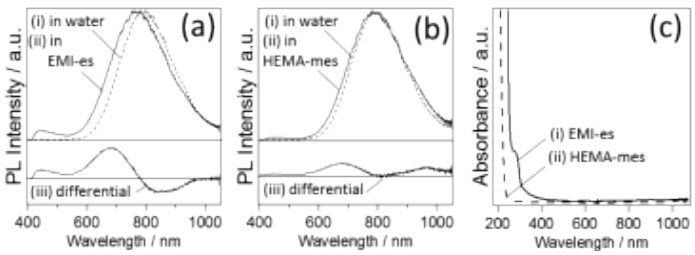

Figure S2. (a) PL spectra of (i) MES-AIS NPs in water (dotted line), (ii) MES-AIS NPs in EMI-es (solid line), and (iii) their differential spectrum. (b) PL spectra of (i) MES-AIS NPs in water (dotted line), (ii) MES-AIS NPs in HEMA-mes (solid line), and (iii) their differential spectrum. (c) Absorption spectra of (i) EMI-es (solid line), and (ii) HEMA-mes(dotted line). From the differential spectra in (a), (b), and the absorption spectrum in (c), PL property of ILs could be confirmed around 400-550 nm. Since the PL properties of the AIS NPs were only changed as a small peak-shifting and/or a small peak-broadening, the PL property of ILs did not interfere the PL property of the AIS NPs significantly by replacing the solvents from water to ILs.

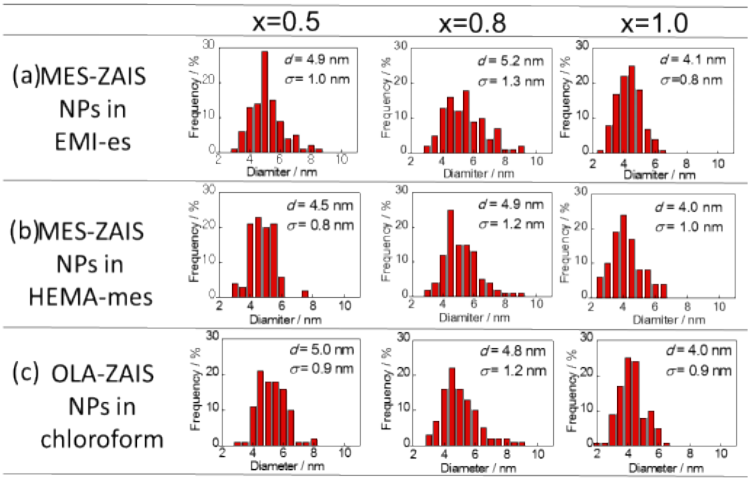

Figure S3. Particle size distributions of ZAIS NPs (x=0.5, 0.8) and AIS NPs (x=1.0) capped with MES in (a) EMI-es, (b) HEMA-mes, and (c) the NPs capped with OLA in chloroform. All the data were estimated from TEM observations, observed before the experiments on the PL stability enhancement.

Highlights in "Improvement of Photoluminescence Stability of ZnS-$AgInS_2$ Nanoparticles through Interactions with Ionic Liquids" written by S. Suzuki and T. Torimoto et al.

- ZnS-$AgInS_2$ nanoparticles dispersed in ionic liquids were prepared.
- Photoluminescence (PL) stability of these nanoparticles was highly improved.
- The PL emission was observed after UV-light irradiation over 80 h.
- The highest record of PL stability was exceeding 390 h.
- Ligand stabilization via electrostatic interaction was proposed for the mechanism.